An Experimental and Computational Study of the Reaction between Pent-3-en-2-yl Radicals and Oxygen Molecules: Switching from Pure Stabilisation to Pure Decomposition with Increasing Temperature

Timo T. Pekkanen[a], Laszlo Valkai[a], Satya P. Joshi[a], György Lendvay[b], Petri Heinonen[a], Raimo S. Timonen[a], Arkke J. Eskola[a,*]

[a] *Department of Chemistry, University of Helsinki, P.O. Box 55 (A.I. Virtasen aukio 1), 00014 Helsinki, Finland*
[b] *Institute of Materials and Environmental Chemistry, Research Centre for Natural Sciences, Magyar Tudósok krt. 2., Budapest H-1117, Hungary*

Supplemental Material

---

*Corresponding author:
Email address: arkke.eskola@helsinki.fi (Arkke J. Eskola)

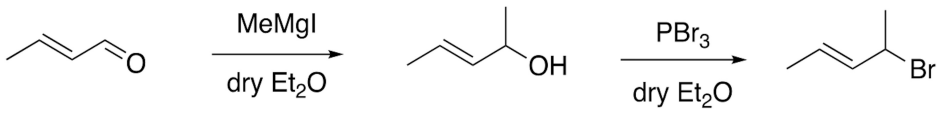

Figure S1: The reaction scheme of 4-bromopent-2-ene synthesis.

1. Synthesis

The radical was precursor, 4-bromopent-2-ene, was synthesised as described in the literature [1]. The NMR spectra were recorded on Varian INOVA 500 MHz or Bruker Avance Neo 400 NMR spectrometers. The chemical shifts are given in ppm using the solvent signal for calibration of the ppm scale.

1.1. Pent-3-en-2-ol

Methyl iodide (12.5 ml, 0.201 mol) was added drop-wise to the magnesium turnings (5,0 g, 0.206 mol) in dry ethyl ether (100 ml). The reaction was stirred for an additional 15 min with a magnetic stirrer after the vigorous reflux had ceased. Crotonaldehyde (16.5 ml, 0.20 mol) was added via a dropping funnel. Stirring was continued overnight at room temperature under Argon. The reaction was quenched by pouring it into 1:1 mixture of 2 M H_2SO_4 solution and ice. The aqueous layer was extracted twice with ethyl ether. The combined organic phases were washed with a saturated $NaHCO_3$ solution and dried over anhydrous K_2CO_3. The solvent was evaporated, and the product was purified by distillation under reduced pressure (64 °C, 65 mmHg). The yield was 10.87 g, 61 %. ^{1}H-NMR (400 MHz, $CDCl_3$) δ 5.74–5.58 (m, 1H), 5.53 (m, 1H), 4.30–4.19 (m, 1H), 1.74–1.64 (m, 3H), 1.24 (d, $J = 6.4$ Hz, 3H).

1.2. 4-bromopent-2-ene

Pent-3-en-ol (10.8 g, 0.125 mol) was dissolved in dry ethyl ether (80 ml) at 0 °C under Argon. Phosphorous tribromide (4.0 ml, 0.042 mol) was added through a septum and the reaction mixture was allowed to warm to room temperature. After a reaction time of 1.5 hours, the reaction was diluted with ethyl ether (100 ml) and the organic phase washed with ice-cold water and brine. The ether layer was dried over $MgSO_4$ and the solvent was evaporated. Distillation under reduced pressure ($61 - 63$ °C/90 mmHg) gave 11.95 g (63 %) of product that had an $E : Z$ isomer ratio of 11 : 1. (E)-isomer: ^{1}H-NMR (500 MHz, $CDCl_3$) δ 5.83–5.64 (m, 2H), 4.70 (m, 1H),

1.78 (d, J = 6.7 Hz, 3H), 1.71 (d, J = 5.0 Hz, 3H). ^{13}C-NMR (125 MHz, $CDCl_3$) δ 134.5, 127.3, 50.5, 26.4, 17.5 (Z)-isomer: 5.7 (m, 1H), 5.5 (m, 1H), 5.0 (m, 1H), 1.79 - 1.70 (m, 6H). ^{13}C-NMR (125 MHz, $CDCl_3$) δ 133.7, 126.8, 44.5, 27.0, 17.8.

References

[1] S. Désert, P. Metzner and M. Ramdani, *Tetrahedron*, 1992, **48**, 10315–10326.

[2] V. D. Knyazev and I. R. Slagle, *J. Phys. Chem. A*, 1998, **102**, 8932–8940.

Table S1: The experimental conditions and results of $CH_3-CH=CH=CH-CH_3 + O_2$ bimolecular rate coefficient measurements. The reported uncertainties are standard errors (1σ).

T (K)	p (Torr)	[M] (10^{16} cm^{-3})	[Pr][a] (10^{11} cm^{-3})	[O_2] (10^{12} cm^{-3})	k' [b] (s^{-1})	k_w[c] (s^{-1})	k_w[d] (s^{-1})	$k(R^\bullet + O_2)$[e] (10^{-12} cm^3 s^{-1})
238[f,j,l]	0.37	1.49	11	12.5 – 56.4	40.3 – 160	5.59 ± 1.11	7.82 ± 4.71	2.73 ± 0.16
238[f,j,l]	0.38	1.54	10	11.8 – 39.3	47.4 – 142	9.76 ± 3.02	9.65 ± 1.59	3.41 ± 0.07
238[f,j,l]	0.62	2.50	10	12.2 – 50.3	46.6 – 168	4.39 ± 1.05	7.14 ± 2.88	3.28 ± 0.11
238[f,j,l]	0.80	3.25	8.6	9.29 – 42.5	39.0 – 178	10.3 ± 2.2	12.0 ± 6.2	4.01 ± 0.29
238[f,j,l]	0.81	3.29	7.00	12.1 – 38.6	50.1 – 138	4.10 ± 1.13	5.86 ± 3.11	3.65 ± 0.16
238[g,j,l]	1.46	5.91	10	15.6 – 32.8	80.6 – 144	15.9 ± 1.7	16.1 ± 3.2	3.95 ± 0.16
238[g,j,l]	3.06	12.4	13	15.2 – 30.8	87.1 – 161	21.2 ± 1.9	19.4 ± 5.1	4.40 ± 0.26
268[f,j,l]	0.41	1.46	11	17.9 – 54.2	38.8 – 100	2.34 ± 1.62	3.31 ± 1.78	1.77 ± 0.06
268[f,j,l]	0.69	2.48	6.8	11.9 – 70.1	28.8 – 157	3.93 ± 0.92	3.40 ± 2.94	2.10 ± 0.08
268[f,j,l]	0.89	3.20	9.4	11.9 – 49.3	31.9 – 131	3.97 ± 0.87	3.98 ± 2.09	2.48 ± 0.07
268[g,j,l]	1.72	6.20	42	21.5 – 72.9	76.8 – 191	11.7 ± 0.9	16.2 ± 4.6	2.48 ± 0.11
268[g,j,l]	3.54	12.8	20	18.4 – 67.8	76.7 – 234	12.0 ± 1.2	14.5 ± 2.8	3.28 ± 0.09
298[f,j,l]	0.46	1.49	6.8	17.7 – 96.7	20.6 – 121	3.40 ± 0.81	1.25 ± 3.16	1.18 ± 0.06
298[f,j,l]	1.01	3.26	7.7	19.5 – 60.0	28.9 – 95.9	1.47 ± 0.65	0.51 ± 1.67	1.56 ± 0.05
298[g,j,l]	1.91	6.17	30	26.3 – 102	56.9 – 203	15.6 ± 1.3	14.4 ± 3.0	1.84 ± 0.06
304[h,k,l]	2.87	9.12	3.6	14.9 – 62.9	42.8 – 144	10.9 ± 1.5	12.1 ± 2.3	2.18 ± 0.08
298[g,h,l]	3.94	12.8	17	25.5 – 75.3	71.4 – 188	12.5 ± 1.0	11.7 ± 1.4	2.31 ± 0.03
304[i,k,m]	0.49	1.57	94	22.9 – 85.1	52.5 – 147	13.8 ± 1.3	15.6 ± 4.2	1.53 ± 0.08
304[i,k,m]	0.79	2.50	66	16.3 – 58.4	39.7 – 118	9.37 ± 1.50	9.08 ± 1.14	1.83 ± 0.04
304[i,k,m]	1.20	3.80	100	17.0 – 47.4	46.9 – 110	10.8 ± 1.3	11.4 ± 1.3	2.09 ± 0.05
304[h,k,m]	1.40	4.46	18	15.5 – 52.0	47.9 – 124	14.7 ± 1.0	15.8 ± 1.9	2.10 ± 0.06
551[h,k,l]	2.0 – 4.6	–	8.3	$(9.36 - 38.5) \cdot 10^3$	24.1 – 38.0	12.9 ± 1.3	21.4 ± 1.1	$(4.30 \pm 0.41) \cdot 10^{-4}$
601[h,k,l]	2.5 – 5.6	–	7.4	$(4.80 - 41.7) \cdot 10^3$	22.0 – 53.7	13.4 ± 1.4	18.3 ± 2.9	$(8.14 \pm 0.95) \cdot 10^{-4}$
651[h,k,l]	2.5 – 5.5	–	8.5	$(5.78 - 42.0) \cdot 10^3$	26.1 – 60.7	17.8 ± 1.2	23.4 ± 2.6	$(8.82 \pm 0.97) \cdot 10^{-4}$
676[h,k,l]	2.5 – 5.1	–	6.8	$(6.60 - 32.9) \cdot 10^3$	37.6 – 75.0	21.2 ± 1.9	29.6 ± 2.3	$(14.0 \pm 0.93) \cdot 10^{-4}$
699[h,k,l]	2.5 – 5.7	–	8.1	$(5.61 - 38.4) \cdot 10^3$	36.3 – 112	21.3 ± 2.0	25.7 ± 2.5	$(22.1 \pm 1.0) \cdot 10^{-4}$
752[h,k,l]	2.5 – 5.9	–	6.6	$(6.61 - 39.5) \cdot 10^3$	39.0 – 113	17.4 ± 2.8	28.3 ± 5.5	$(21.0 \pm 2.1) \cdot 10^{-4}$

[a] Radical precursor is (E/Z)-4-bromopent-2-ene (11 : 1) kept between -10 °C and -25 °C. KrF (248 nm) laser used for photolysis.

[b] The pseudo-first-order rate coefficient $k' = k_w + k[O_2]$.

[c] Average of measured wall rates. The wall rate is the pent-3-en-2-yl decay rate in the absence of O_2.

[d] Wall rate determined from the linear fit y-axis intercept.

[e] Experimentally determined bimolecular rate coefficient.

[f] Reactor: $d = 1.7$ cm, Stainless Steel/Halocarbon wax

[g] Reactor: $d = 0.80$ cm, Stainless Steel/Halocarbon wax

[h] Reactor: $d = 0.85$ cm, Quartz/Boric Oxide

[i] Reactor: $d = 1.7$ cm, Pyrex/Polydimethylsiloxane

[j] N_2/Sapph

[k] N_2/Quartz

[l] He bath gas

[m] N_2 bath gas

Table S2: The experimental conditions and results of the $R^{\bullet} + O_2 \rightleftharpoons RO_2^{\bullet}$ equilibration measurements. The reported uncertainties are evaluated using error propagation. The averaging scheme of Knyazev and Slagle[2] is used to obtain the values for $k_w^{(P)}$, k_f, k_r, and $\ln(K)$.

T (K)	p (Torr)	[M] (10^{16} cm^{-3})	[O_2] (10^{-12} cm^{-3})	k_w [a] (s^{-1})	$k_w^{(P)}$ [b] (s^{-1})	k_f [c] (10^{-13} cm^3 s^{-1})	k_r [d] (s^{-1})	$\ln(K)$ [e]
326[f,h,i]	0.99	2.94	350	11.4 ± 1.1	15.5 ± 1.1	9.41 ± 0.85	15.8 ± 28.4	14.10 ± 1.80
331[f,h,i]	1.02	2.97	212	9.56 ± 1.10	13.5 ± 4.7	9.25 ± 0.85	15.3 ± 17.6	14.09 ± 1.15
337[f,h,i]	0.98	2.80	217	13.2 ± 1.2	19.9 ± 4.5	8.94 ± 0.96	31.5 ± 24.2	13.32 ± 0.78
344[f,h,i]	0.99	2.69	201	11.5 ± 1.0	13.3 ± 3.3	7.13 ± 0.77	32.4 ± 18.6	13.05 ± 0.58
348[f,h,i]	0.99	2.76	199	11.4 ± 0.8	9.10 ± 2.46	7.37 ± 0.80	43.1 ± 19.5	12.78 ± 0.46
348[f,h,i]	0.99	2.76	338	11.4 ± 0.8	11.4 ± 2.5	6.12 ± 0.58	36.5 ± 21.0	12.76 ± 0.58
352[g,h,i]	2.87	7.86	151	14.3 ± 1.0	24.1 ± 6.7	10.6 ± 0.2	98.6 ± 54.0	12.31 ± 0.58
352[g,h,i]	2.88	7.89	314	14.3 ± 1.0	17.9 ± 3.9	7.21 ± 0.90	66.8 ± 43.2	12.31 ± 0.66
352[g,h,i]	2.91	7.99	648	14.3 ± 1.0	18.4 ± 3.8	5.79 ± 0.70	97.7 ± 67.5	11.71 ± 0.70
352[g,h,i]	2.95	8.10	640	14.4 ± 0.8	16.7 ± 2.1	6.00 ± 0.45	85.6 ± 37.2	11.88 ± 0.44
353[f,h,i]	0.49	1.34	290	10.7 ± 1.2	13.5 ± 3.6	5.72 ± 0.93	48.3 ± 30.7	12.40 ± 0.66
353[f,h,i]	0.98	2.68	289	10.7 ± 1.2	9.74 ± 1.22	6.92 ± 0.91	45.3 ± 29.7	12.65 ± 0.66
353[f,h,i]	2.01	5.49	289	10.7 ± 1.2	10.9 ± 3.2	7.10 ± 0.99	61.7 ± 43.3	12.37 ± 0.72
359[f,h,i]	1.50	4.02	288	9.95 ± 1.25	6.99 ± 3.77	3.93 ± 0.75	61.6 ± 37.2	11.77 ± 0.63
359[g,h,i]	1.93	5.19	386	17.8 ± 1.1	28.8 ± 4.8	6.48 ± 0.76	104 ± 46	11.74 ± 0.46
360[g,h,j]	1.86	4.98	200	19.5 ± 1.4	16.4 ± 9.9	3.30 ± 0.11	56.9 ± 43.0	11.66 ± 0.82
360[g,h,i]	3.87	10.4	374	18.7 ± 1.1	27.4 ± 5.8	6.91 ± 0.10	115 ± 62	11.70 ± 0.56
365[f,h,i]	1.49	3.93	363	9.70 ± 0.78	9.06 ± 2.46	5.29 ± 0.83	125 ± 53	11.33 ± 0.45
371[f,h,i]	1.50	3.89	395	9.94 ± 0.91	8.44 ± 2.69	4.01 ± 0.73	144 ± 56	10.90 ± 0.43
376[f,h,i]	1.50	3.85	406	8.16 ± 0.78	9.66 ± 4.95	2.87 ± 0.93	212 ± 104	10.17 ± 0.59

[a] Average of measured wall rates. The wall rate is the pent-3-en-2-yl decay rate in the absence of O_2.

[b] An "average" value for the wall rates of the peroxyl adducts.

[c] An "average" forward rate coefficient.

[d] An "average" reverse rate coefficient.

[e] An "average" equilibrium constant. The standard states have been chosen as pure ideal gas at $p^{\ominus} = 1$ bar at the temperature of interest.

[f] Reactor: $d = 1.7$ cm, Quartz/Polydimethylsiloxane

[g] Reactor: $d = 0.85$ cm, Quartz/Boric Oxide

[h] N_2/Quartz

[i] He bath gas

[j] N_2 buffer gas

Table S3: Zero-kelvin reaction enthalpies ($\Delta_r H_0^{\ominus}$) for the stationary points on the potential surface of the $CH_3-CH=CH=CH-CH_3 + O_2$ reaction at various levels of theory. The energies are in kJ mol^{-1}.

Species	$\sigma_{ext} \cdot \sigma_{int}/m_{opt}$ [a]	ΔZPE	MN15/Def2TZVP	DLPNO-ROHF-CCSD(T1)/CBS[b]	CASPT2/CBS[c]	Fitted
R	$2 \cdot 9/1$, $2 \cdot 1/1$	0	0	0 (0.019, 0.017)		
Int1E	$1 \cdot 9/2$	16.96	-90.27	-79.91 (0.022)	**-83.08**[c] (0.74)	-83.08
Int1Z	$1 \cdot 9/2$	17.51	-86.35	-74.18 (0.022)	**-77.35**[c] (0.74)	-77.35
Int2	$1 \cdot 6/2$	13.17	-85.70	-77.54 (0.019)	-75.94 (0.74)	
P1E	$1 \cdot 3/1$, $1 \cdot 1/1$	3.583	-13.91	-14.87 (0.011, 0.030)		
P1Z	$1 \cdot 3/1$, $1 \cdot 1/1$	4.339	-8.295	-8.775 (0.011, 0.030)		
P2RR		2.591	-102.2	-99.37 (0.011, 0.016)		
P2SR		2.974	-98.44	-95.10 (0.011, 0.016)		
ts1EP1E	$1 \cdot 3/2$	0.8431	21.83	32.56 (0.027)	10.84 (0.73)	13.42
ts1ZP1Z	$1 \cdot 3/2$	1.401	26.67	37.81 (0.027)	15.00 (0.73)	17.57
ts1Z2a	$1 \cdot 3/2$	4.393	11.02	26.20 (0.020)	23.09 (0.73)	
ts1Z2b	$1 \cdot 3/2$	3,365	10.78	24.67 (0.021)	18.04 (0.73)	
ts1Z2c	$1 \cdot 3/2$	4.141	9.967	24.10 (0.020)	20.44 (0.73)	
ts1Z2d	$1 \cdot 3/2$	3.686	21.69	36.72 (0.022)	31.20 (0.73)	
ts2P2RR	$1 \cdot 3/2$	5.254	2.195	5.975 (0.037)	-18.49 (0.73)	
ts2P2SR	$1 \cdot 3/2$	5.896	5.324	9.500 (0.037)	-15.10 (0.73)	
Int3RR		17.52	-93.67	-74.50 (0.013)	-77.86 (0.75)	
Int3SR		17.23	-94.27	-75.61 (0.013)	-79.02 (0.75)	
ts1E3RR		13.42	19.04	30.44 (0.022)	19.48 (0.74)	
ts1E3SR		13.57	19.01	31.69 (0.022)	20.83 (0.74)	
ts1Z3RR		14.00	34.29	49.35 (0.024)	36.44 (0.74)	
ts1Z3SR		14.27	34.67	49.52 (0.024)	36.38 (0.74)	
ts3RRP3RR		9.099	34.00	45.30 (0.040)	27.96 (0.74)	
ts3RRP3SR		11.04	44.57	52.84 (0.037)	31.63 (0.74)	
ts3SRP3RR		9.904	39.92	50.38 (0.039)	31.87 (0.50)	
ts3SRP3SR		10.47	37.88	48.44 (0.038)	27.78 (0.74)	
P3RR		4.521	-162.2	-151.1 (0.018, 0.014)		
P3SR		4.526	-161.7	-150.7 (0.018, 0.014)		

[a] Here σ_{ext} and σ_{int} are the external and internal rotational symmetry numbers, respectively, and m_{opt} is the optical symmetry number.

[b] The tightPNO settting was employed in the DLPNO calculations. The values in the parentheses are the T1 diagnostics.

[c] The CASPT2 values are expressed relative to optimized the Int1E and Int1Z well depths (see main text). The values in the parentheses are the reference weights.

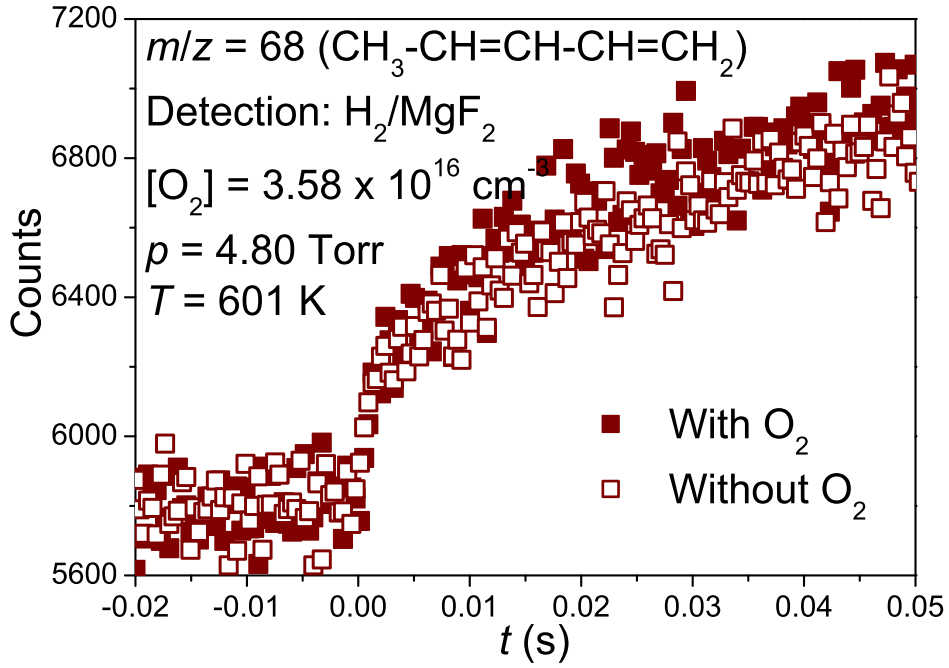

Figure S2: Measured traces at $m/z = 68$ in the presence and absence of O_2

Table S4: The modified Arrhenius parameters for the product channels.

$k(T) = AT^m \mathrm{e}^{-E_\mathrm{a}/RT}$			
Reaction	A ($\mathrm{cm}^3\ \mathrm{s}^{-1}$)	m	E_a ($\mathrm{cal\ mol}^{-1}$)
R $\longrightarrow$ P1E	$1.66 \cdot 10^{-18}$	1.26	3030
R $\longrightarrow$ P1Z	$2.88 \cdot 10^{-18}$	1.22	3710
R $\longrightarrow$ P2RR	$1.02 \cdot 10^{-29}$	4.02	-2500
R $\longrightarrow$ P2SR	$5.27 \cdot 10^{-30}$	4.08	-1750

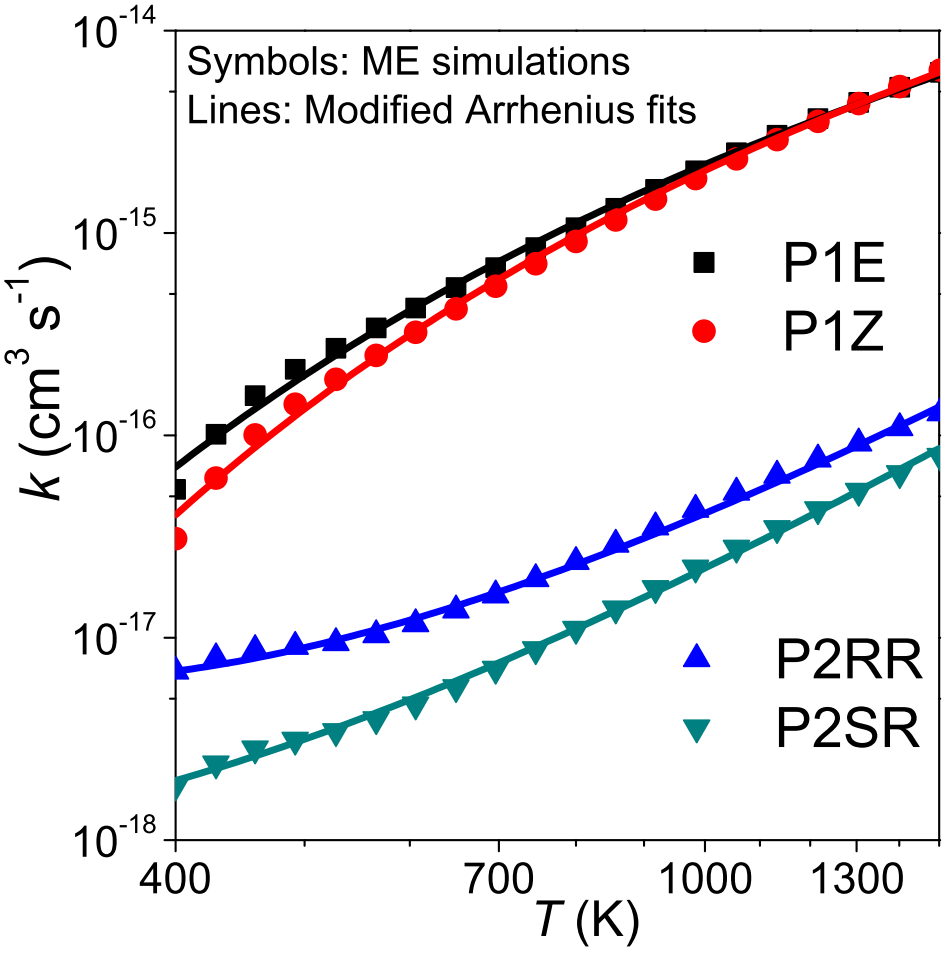

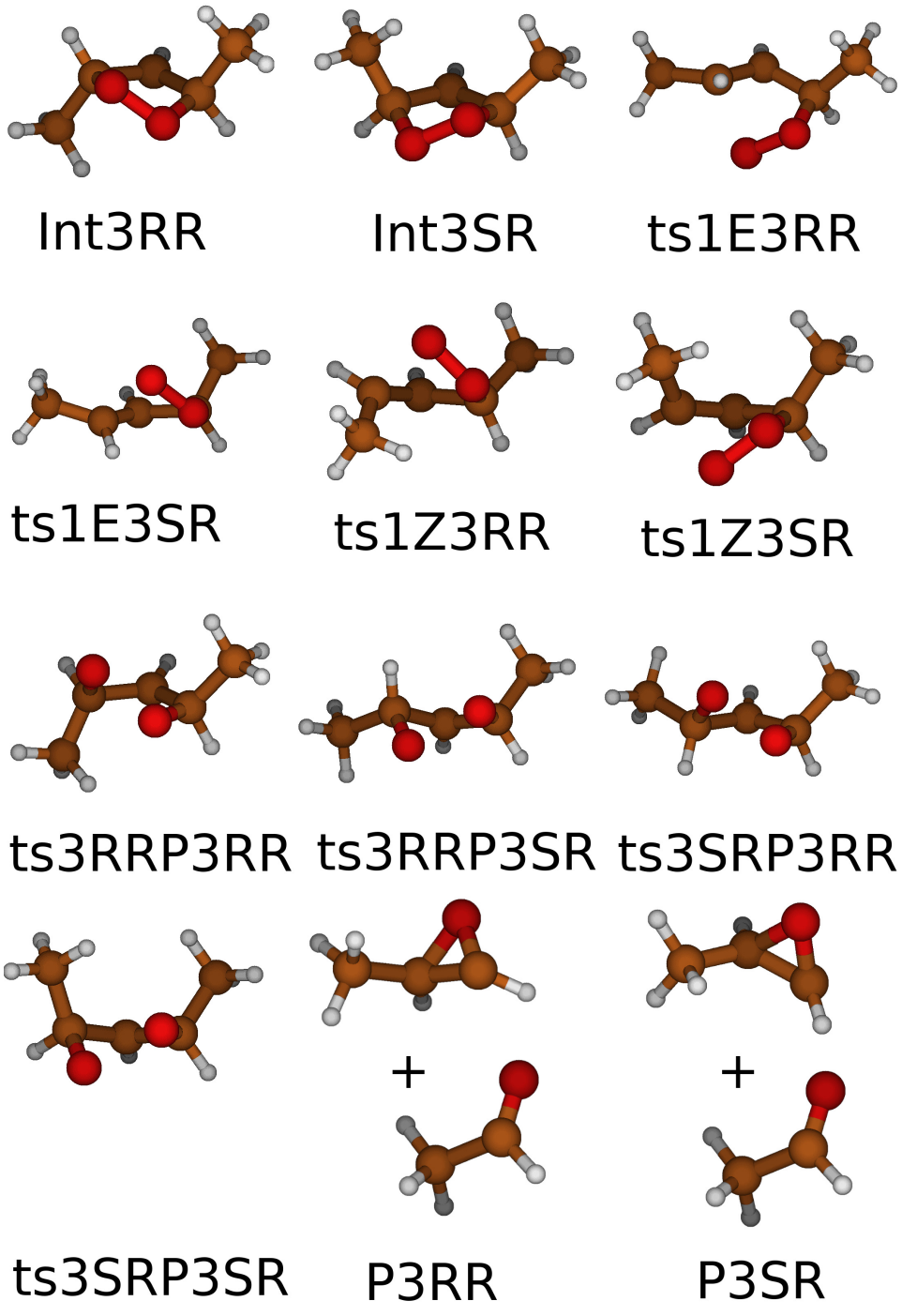

Figure S3: The stationary points for product channel P3.

2. High-Temperature Bimolecular Plots

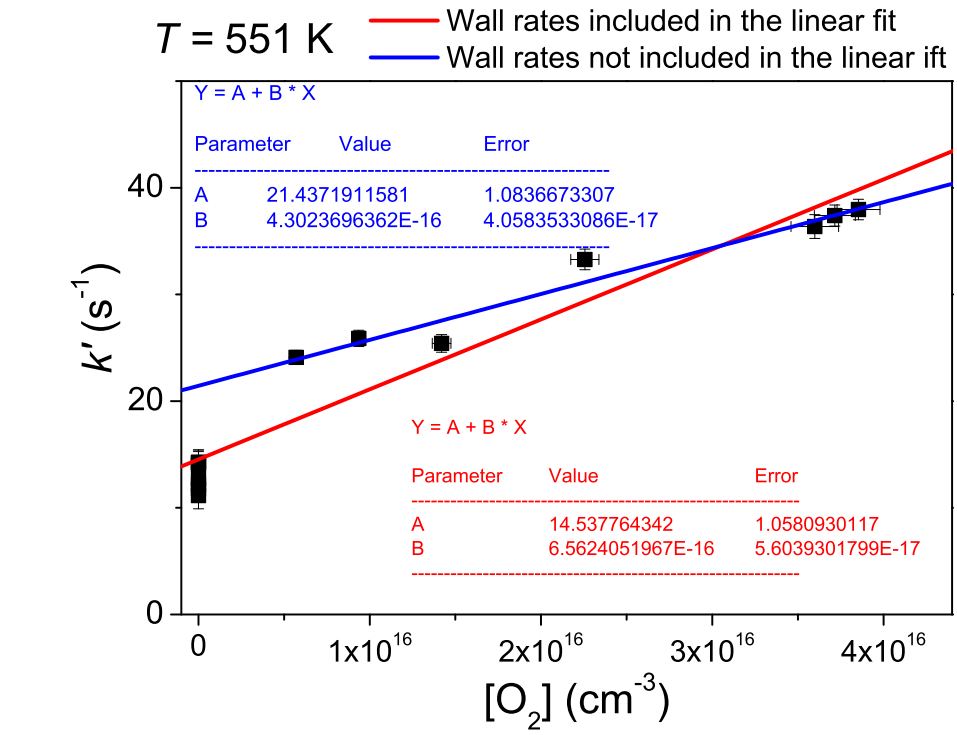

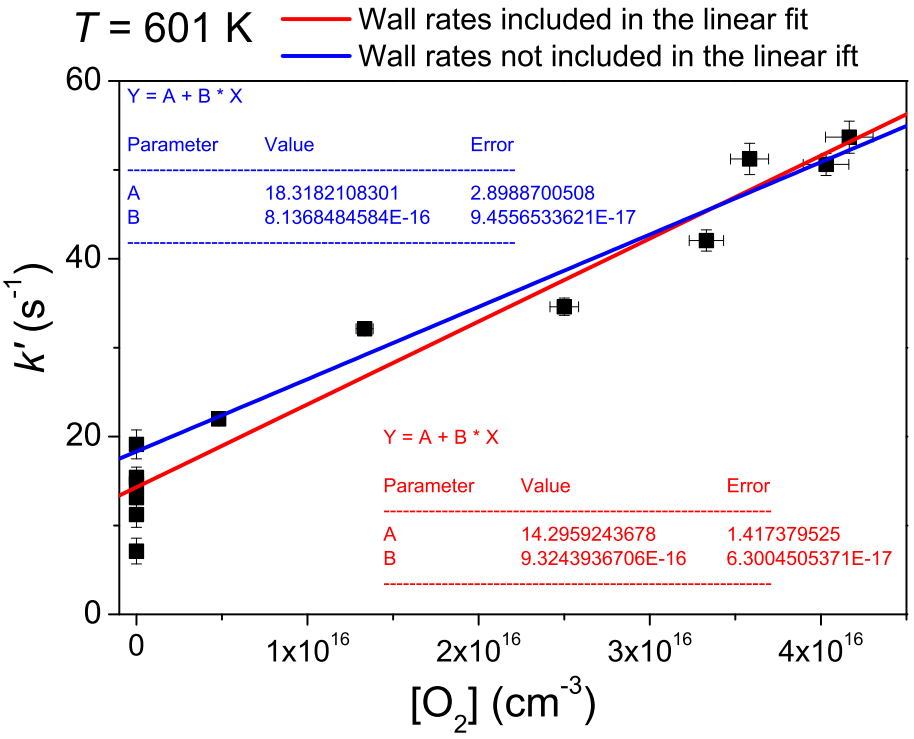

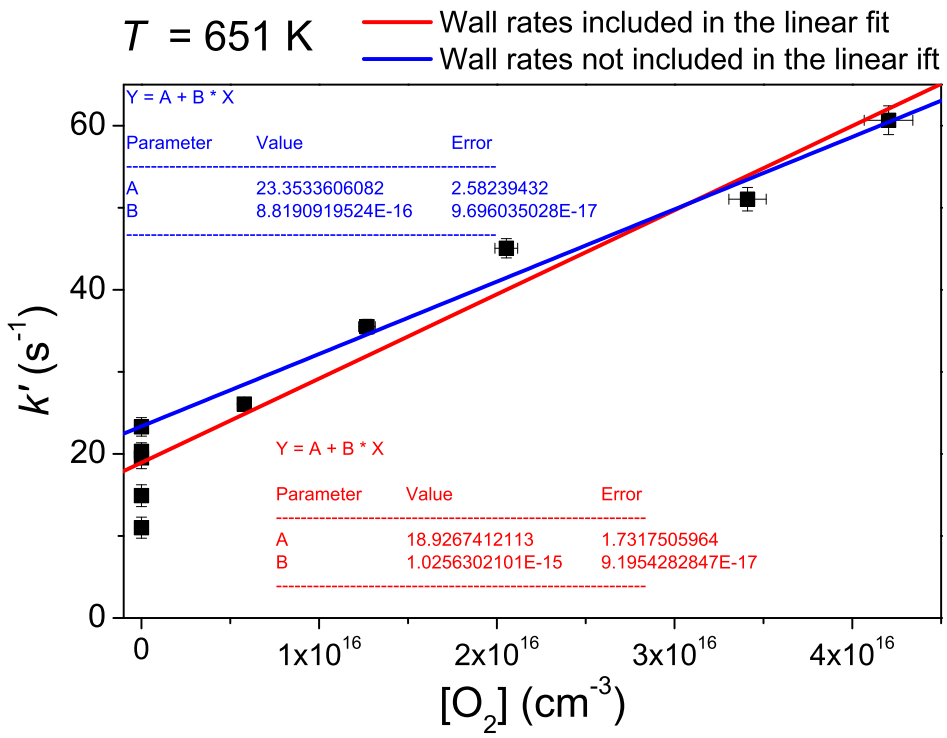
T = 651 K
Wall rates included in the linear fit
Wall rates not included in the linear ift
Y = A + B * X
Parameter Value Error
A 23.3533606082 2.58239432
B 8.8190919524E-16 9.696035028E-17
Y = A + B * X
Parameter Value Error
A 18.9267412113 1.7317505964
B 1.0256302101E-15 9.1954282847E-17
k' (s-1)
[O2] (cm-3)
0
20
40
60
0
1x10^16
2x10^16
3x10^16
4x10^16

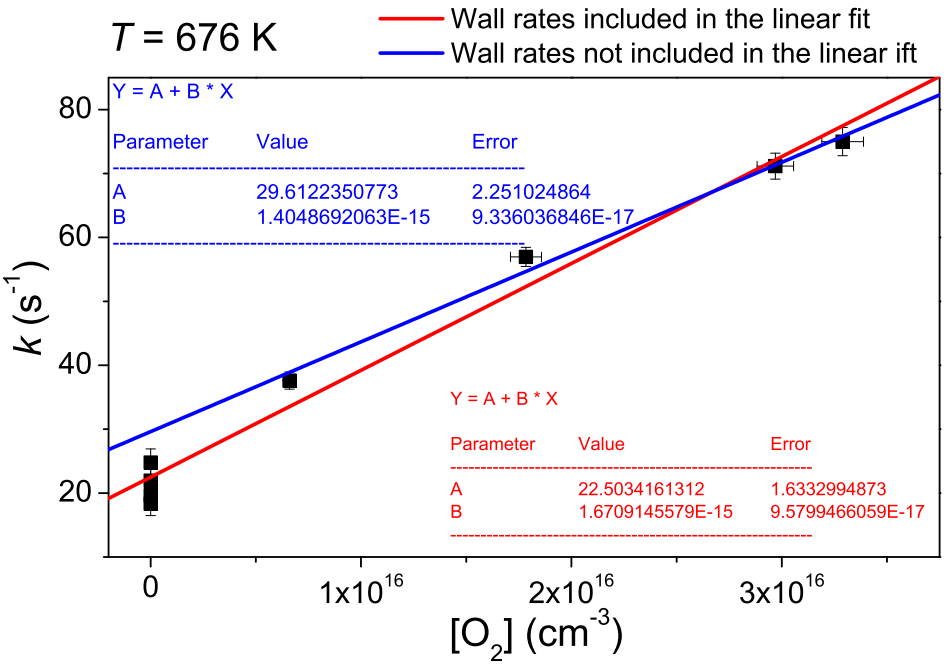
T = 676 K
Wall rates included in the linear fit
Wall rates not included in the linear ift
Y = A + B * X
Parameter Value Error
A 29.6122350773 2.251024864
B 1.4048692063E-15 9.336036846E-17
Y = A + B * X
Parameter Value Error
A 22.5034161312 1.6332994873
B 1.6709145579E-15 9.5799466059E-17
k (s-1)
[O2] (cm-3)
20
40
60
80
0
1x10^16
2x10^16
3x10^16

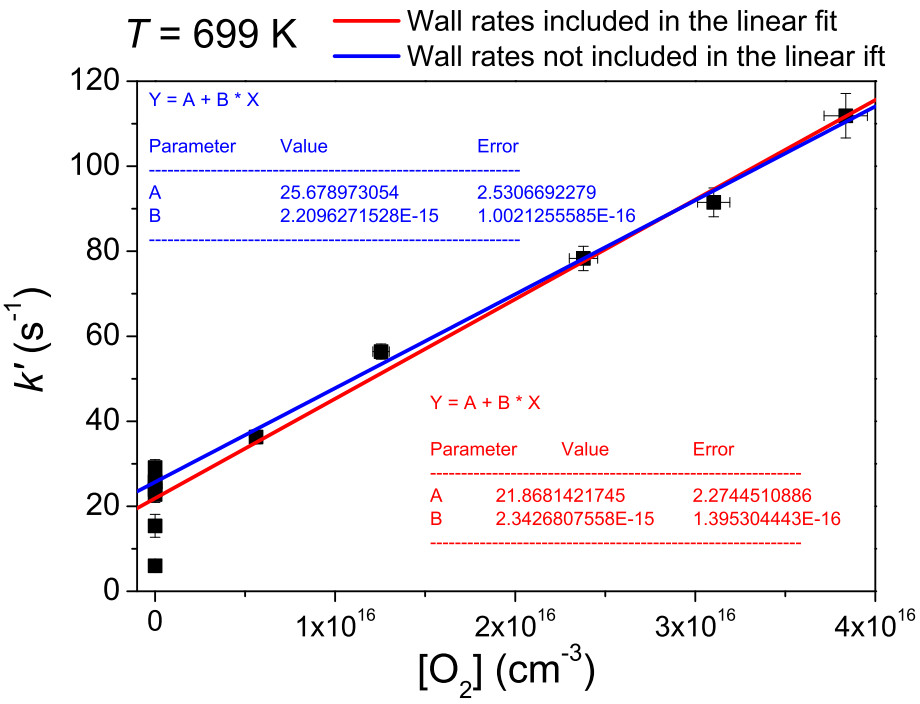
T = 699 K
Wall rates included in the linear fit
Wall rates not included in the linear ift
Y = A + B * X
Parameter Value Error
A 25.678973054 2.5306692279
B 2.2096271528E-15 1.0021255585E-16
Y = A + B * X
Parameter Value Error
A 21.8681421745 2.2744510886
B 2.3426807558E-15 1.395304443E-16
k' (s-1)
[O2] (cm-3)
0
20
40
60
80
100
120
0
1x10^16
2x10^16
3x10^16
4x10^16

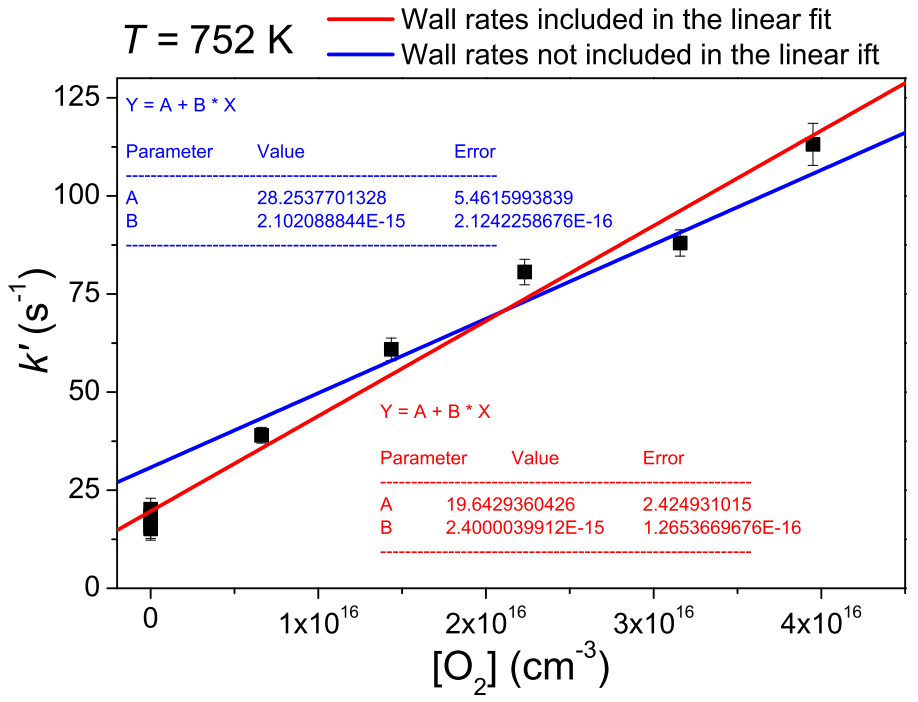
T = 752 K
Wall rates included in the linear fit
Wall rates not included in the linear ift
Y = A + B * X
Parameter Value Error
A 28.2537701328 5.4615993839
B 2.102088844E-15 2.1242258676E-16
Y = A + B * X
Parameter Value Error
A 19.6429360426 2.424931015
B 2.4000039912E-15 1.2653669676E-16
k' (s-1)
[O2] (cm-3)
0
25
50
75
100
125
0
1x10^16
2x10^16
3x10^16
4x10^16